

Invisible Z-boson decays at e^+e^- colliders

Marcela Carena, André de Gouvêa, and Ayres Freitas
Theoretical Physics Division, Fermilab, P.O. Box 500, Batavia, Illinois 60510, USA

Michael Schmitt

Northwestern University, Department of Physics & Astronomy, 2145 Sheridan Road, Evanston, Illinois 60208, USA
 (Received 22 August 2003; published 30 December 2003)

The measurement of the invisible Z-boson decay width at e^+e^- colliders can be done “indirectly,” by subtracting the Z-boson visible partial widths from the Z-boson total width, or “directly,” from the process $e^+e^- \rightarrow \gamma\nu\bar{\nu}$. Both procedures are sensitive to different types of new physics and provide information about the couplings of the neutrinos to the Z boson. At present, measurements at CERN LEP and CHARM II are capable of constraining the left-handed $Z\nu\bar{\nu}$ coupling, $0.45 \leq g_L \leq 0.5$, while the right-handed one is only mildly bounded, $|g_R| \leq 0.2$. We show that measurements at a future e^+e^- linear collider at different center-of-mass energies, $\sqrt{s} = m_Z$ and $\sqrt{s} \approx 170$ GeV, would translate into a markedly more precise measurement of the $Z\nu\bar{\nu}$ couplings. A statistically significant deviation from standard model predictions will point toward different new physics mechanisms, depending on whether the discrepancy appears in the direct or the indirect measurement of the invisible Z width. We discuss some scenarios which illustrate the ability of different invisible Z-boson decay measurements to constrain new physics beyond the standard model.

DOI: 10.1103/PhysRevD.68.113007

PACS number(s): 13.38.Dg

I. INTRODUCTION

The four CERN e^+e^- collider LEP collider experiments have performed several precise measurements of the properties of the Z boson [1–4], the heavy, neutral partner of the W boson and the photon. These measurements are part of the evidence that the standard model (SM) of the electroweak interactions works extremely well, up to energies of several hundred GeV. One of these measurements is associated with the “invisible Z-boson width” (invisible Z width). Assuming that the SM is correct, this measurement can be translated into a count of the number of neutrino species. The current value of the invisible Z width agrees quite well with the SM expectation that there are three very light ($m_\nu \ll 1$ GeV) neutrino species. This is often interpreted as evidence that the SM contains three and only three families of fermionic fields, meaning that there is no fourth sequential generation. It is remarkable that this result is in agreement with cosmological constraints on the number of relativistic species around the time of big bang nucleosynthesis, which seem to indicate the existence of three very light neutrino species [5].

It is interesting to note that the LEP result is precise enough to probe whether the “number of neutrinos” N_ν deviates slightly from three. Indeed, it is often quoted that the most precise LEP numbers can be translated into $N_\nu = 2.9841 \pm 0.0083$ [2], about two sigma away from the SM expectation, $N_\nu = 3$. While not statistically significant, this result has invited theoretical speculations, some of which involve suppressing the $Z\nu\bar{\nu}$ couplings with respect to the SM value.

More recently, the NuTeV Collaboration presented a measurement of $\sin^2\theta_W$ obtained from neutrino-nucleon scattering [6]. This result overshoots the SM prediction by about three sigma [$\sin^2\theta_W = 0.2277 \pm 0.0016$ (NuTeV) versus $\sin^2\theta_W = 0.2227 \pm 0.0004$ (SM prediction), see [6]]. One pos-

sible explanation of this “NuTeV anomaly” is that the $Z\nu\bar{\nu}$ couplings are suppressed (by a factor $\rho_0 = 0.9941 \pm 0.0021$ [7]) with respect to their SM values [6–9].

In light of these two either statistically weak (the invisible Z width at LEP) or controversial (the NuTeV anomaly) discrepancies, the particle physics community would profit from other independent, precise measurements of the $Z\nu\bar{\nu}$ couplings. We argue that a linear collider experiment, capable of taking data around and above the Z-boson mass, can provide useful, precise, and, more importantly, “different” measurements with invisible Z-boson decays.

One reason for this is that the most precise LEP measurement of the invisible Z width is *indirect*, in the sense that it is determined by subtracting the Z-boson visible partial widths from the Z-boson total width. We argue that at a (much) higher statistics linear collider experiment a competitive, *direct* measurement of the invisible Z-boson width can be obtained from the process $e^+e^- \rightarrow \gamma\nu\bar{\nu}$ by counting events with a photon plus missing energy.

The indirect and direct measurements of the invisible Z width are sensitive to different types of physics beyond the SM in different ways. While in some scenarios (e.g. modified $Z\nu\bar{\nu}$ couplings) the two results should be identical (and, perhaps, different from SM expectations), in other scenarios (e.g. a nonzero $\gamma\nu\bar{\nu}$ coupling) the two measurements of the invisible Z-width may disagree.

Furthermore, the very precise LEP result, obtained at center-of-mass energies around the Z-boson mass, is, in practice, only sensitive to a particular combination of the $Z\nu\bar{\nu}$ couplings: $g_L^2 + g_R^2$, where g_L (g_R) is the left-handed (right-handed) $Z\nu\bar{\nu}$ coupling. In the SM, the neutrinos only couple left-handedly to the Z and W bosons, but the “left-handedness” of the $Z\nu\bar{\nu}$ couplings has not been experimentally established with good precision. Some information on

g_L and g_R can be obtained, under a specific set of assumptions, by combining the LEP result with results from neutrino-electron scattering. Furthermore, by looking at $e^+e^- \rightarrow \gamma\nu\bar{\nu}$ at center-of-mass energies above the Z-boson mass, one is sensitive to both $(g_L^2 + g_R^2)$ and g_L separately, thanks to the interference between the s -channel Z-boson exchange and the t -channel W -boson exchange. This means that by analyzing LEP data at center-of-mass energies above the Z-boson mass one can also learn about the individual values of g_L and g_R . A linear collider experiment taking data above the Z-boson mass (at, for example, $\sqrt{s} = 170$ GeV) can perform a more precise (and less model dependent) measurement of g_L and g_R , as will be studied in detail.

This manuscript is organized as follows. In Sec. II, we discuss in some detail the LEP measurements of the invisible Z width, emphasizing the assumptions that are made in order to obtain the precise value of N_ν quoted above. Having done that, we discuss how precisely one should be able to directly measure the invisible Z width at a linear collider operating at center-of-mass energies “around” the Z-boson mass. In Sec. III, we discuss how one should be able to measure the neutrino g_L and g_R couplings separately by taking e^+e^- data at center-of-mass energies higher than the Z-boson mass. We look at current constraints that can be obtained from combining LEP data with data on neutrino-electron scattering, and then examine the existing LEP data collected above the Z-boson mass (LEP II). We proceed to discuss how well a similar procedure can be executed at a linear collider. In Sec. IV, we analyze new physics contributions that would lead to discrepancies between the SM and the “measurements” which are proposed above. A summary of the results and some parting thoughts are presented in Sec. V.

II. THE INVISIBLE Z-BOSON WIDTH AROUND THE Z POLE

The SM predicts that around 20% of the time a Z boson will decay into a $\nu\bar{\nu}$ pair. The neutrino pair cannot be observed directly in collider experiments, meaning that Z bosons decaying in this fashion are “invisible.”

In electron-positron colliders there are two ways of establishing whether these invisible Z boson decays are occurring, and to measure the invisible Z width. One is to directly measure the total Z width, Γ_{tot} , by studying the line shape of the Z boson (this is done by colliding e^+e^- at center-of-mass energies around the Z-boson mass), and measuring its partial decay widths in visible final states, Γ_{vis} , namely charged leptons and hadrons. One can then compute the invisible Z width, Γ_{inv} : $\Gamma_{\text{inv}} = \Gamma_{\text{tot}} - \Gamma_{\text{vis}}$. This procedure is discussed in detail below, in Sec. II A. The other is to look for events where an initial state lepton radiates off a hard photon before annihilating into an s -channel Z boson. When that happens, if the Z boson decays invisibly, the experimentally observed final state is a single photon plus a significant amount of “missing energy” (in summary, $e^+e^- \rightarrow \gamma Z \rightarrow \gamma\nu\bar{\nu}$). This procedure will be discussed in detail in Sec. II B.

A. On the LEP (indirect) measurement of the invisible Z-boson width

At LEP, the invisible Z width is indirectly extracted from the following observables:

(i) $\Gamma_{\text{tot}} = 2.4952 \pm 0.0023$ GeV, the total width of the Z boson¹ and $m_Z = 91.1876 \pm 0.0021$ GeV, the Z-boson pole mass.

(ii) $\sigma_h^0 = 41.541 \pm 0.037$ nb, the hadronic pole cross section, defined as

$$\sigma_h^0 \equiv \frac{12\pi}{m_Z^2} \frac{\Gamma_{ee}\Gamma_{\text{had}}}{\Gamma_{\text{tot}}^2}, \quad (2.1)$$

where Γ_{ee} and Γ_{had} are the partial Z-boson decay widths into an e^+e^- pair and into hadrons respectively.

(iii) $R_\ell = 20.804 \pm 0.050$, 20.785 ± 0.033 , 20.764 ± 0.045 for $\ell = e, \mu, \tau$, respectively, defined as $\Gamma_{\text{had}}/\Gamma_{\ell\ell}$. If one assumes universal Z-boson couplings to charged leptons, $R_\ell = 20.767 \pm 0.025$.

Assuming lepton universality and taking into account the fact that several of the measurements listed above are strongly correlated, one can easily compute the invisible Z width and obtain the LEP result, which is quoted by the Particle Data Group (PDG) [2],

$$\Gamma_{\text{inv}}^{\text{LEP}} = 499.0 \pm 1.5 \text{ MeV}. \quad (2.2)$$

This result is to be compared to the SM prediction,

$$\Gamma_{\text{inv}}^{\text{SM}} = 501.3 \pm 0.6 \text{ MeV}, \quad (2.3)$$

meaning that $\Delta\Gamma_{\text{inv}} \equiv \Gamma_{\text{inv}}^{\text{SM}} - \Gamma_{\text{inv}}^{\text{LEP}} = -2.2 \pm 1.6$ MeV, a 1.4σ effect. This result can also be expressed as an upper bound on additional contributions to the invisible Z width. Numerically, one obtains $\Gamma_{\text{inv}}^{\text{new}} < 2.0$ MeV at the 95% confidence level, assuming that the new physics contributions add incoherently with the neutrino pair production (i.e., $\Gamma_{\text{inv}}^{\text{new}}$ is strictly positive).

In order to obtain the well known 2σ discrepant measurement of the number of neutrinos, one should consider the ratio of partial widths

$$\frac{\Gamma_{\text{inv}}}{\Gamma_{\ell\ell}} \equiv N_\nu \left(\frac{\Gamma_{\nu\nu}}{\Gamma_{\ell\ell}} \right)_{\text{SM}}. \quad (2.4)$$

Equation (2.4) defines what is meant by the “number of neutrinos.” N_ν only agrees with the *de facto* number of neutrinos if both the $Z\ell\bar{\ell}$ and the $Z\nu\bar{\nu}$ couplings have their SM predicted values. The SM prediction for $(\Gamma_{\nu\nu}/\Gamma_{\ell\ell})_{\text{SM}} = 1.9912 \pm 0.0012$ is more precisely known than the individual partial widths, and when compared to the extracted value of $\Gamma_{\text{inv}}/\Gamma_{\ell\ell} = 5.942 \pm 0.016$ yields

$$N_\nu^{\text{LEP}} = 2.9841 \pm 0.0083, \quad (2.5)$$

¹These are the combined values obtained by the LEP Electroweak Working Group [3,4].

the result we alluded to in the Introduction.

The results Eq. (2.2) and Eq. (2.5) imply different consequences for different SM extensions. For example, modified $Z\nu\bar{\nu}$ couplings combined with *identically* modified $Z\ell^+\ell^-$ couplings would ideally lead to a nonzero $\Delta\Gamma_{\text{inv}}$ but to a zero $N_\nu - 3$. Furthermore, given the indirect way that Γ_{inv} is extracted, one should be careful when it comes to defining what $\Delta\Gamma_{\text{inv}}$ is really sensitive to. The observation of a discrepant Γ_{inv} and/or N_ν , does *not* necessarily imply that there is new physics in the neutrino sector or even in the leptonic sector. For example, it is possible that other effects may modify the extracted value of Γ_{tot} , hence inducing a discrepancy between the measured invisible Z width and its SM prediction. This will be further explored in Sec. IV.

We have also extracted the value of the invisible Z width without assuming lepton universality and, using the results presented in [3,4], obtained

$$\Gamma_{\text{inv}}^{LEP}(\text{nonuniversal}) = 497.4 \pm 2.5 \text{ MeV}, \quad (2.6)$$

less precise than the result obtained assuming universality, as expected. In spite of that, $\Delta\Gamma_{\text{inv}}(\text{nonuniversal}) = -3.9 \pm 2.6 \text{ MeV}$, still a 1.5σ deviation, is as significant as the effect obtained assuming universality. This result translates into an upper bound on $\Gamma_{\text{inv}}^{\text{new}} < 3.2 \text{ MeV}$ at the 95% confidence level, assuming that the new physics effect does not interfere with the neutrino-antineutrino final state.

An attempt to extract the number of neutrinos via Eq. (2.4) without charged-lepton universality would be rather peculiar, since one needs to explicitly assume that $\Gamma_{\nu_e\nu_e} = \Gamma_{\nu_\mu\nu_\mu} = \Gamma_{\nu_\tau\nu_\tau}$ in order to relate N_ν to a ‘‘neutrino number.’’ Nonetheless, one can easily extract the value of $\Gamma_{\text{inv}}/\Gamma_{ee}$ and $\Gamma_{\text{inv}}/\Gamma_{\mu\mu}$, and compute, respectively, N_ν^{ee} and $N_\nu^{\mu\mu}$, these being defined via Eq. (2.4) with $\Gamma_{\ell\ell}$ replaced, respectively, by Γ_{ee} and $\Gamma_{\mu\mu}$. We obtain

$$N_\nu^{ee} = 2.978 \pm 0.012, \quad (2.7)$$

$$N_\nu^{\mu\mu} = 2.973 \pm 0.019. \quad (2.8)$$

These are, respectively, 1.8σ and 1.4σ away from the SM prediction of $N_\nu = 3$.

B. (Direct) measurement of the invisible Z-boson width at a linear collider

In the SM, for center-of-mass energies around the Z-boson mass, the dominant contribution to $e^+e^- \rightarrow \gamma + \text{missing energy}$ comes from an intermediate $Z\gamma$ pair, followed by $Z \rightarrow \nu\bar{\nu}$. Other contributions come from t -channel W -boson exchange, plus one photon vertex attached either to the initial state electrons or to the intermediate state charged gauge boson. The leading order Feynman diagrams are depicted in Fig. 1.

The LEP collaborations have measured the cross section for the photon plus missing energy final state. The most precise result comes from the L3 experiment, after analyzing of 100 pb^{-1} of data: $\Gamma_{\text{inv}} = 498 \pm 12 \pm 12 \text{ MeV}$ [10] (the first error is due to statistics, while the second one to systemat-

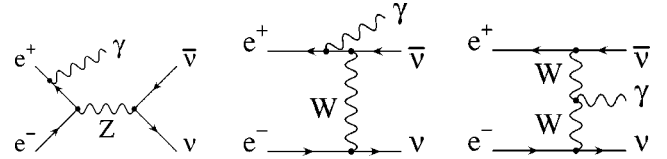


FIG. 1. Leading order Feynman diagrams contributing to $e^+e^- \rightarrow \gamma\nu\bar{\nu}$.

ics). Other LEP collaborations have older results [11–14] (from smaller data samples) with errors, both statistical and systematic, which are two to six times larger. The PDG average is $\Gamma_{\text{inv}} = 503 \pm 16 \text{ MeV}$ [2], dominated by the L3 result [10]. For later comparison, it proves useful to estimate the ultimate sensitivity for LEP (including all four experiments analyzing all the data collected around the Z-boson mass). We do this by naively rescaling the L3 result from 100 pb^{-1} to roughly 500 pb^{-1} . Assuming that both the statistical error and the systematic error will decrease by a factor $\sqrt{500/100}$, we obtain $\delta\Gamma_{\text{inv}} = \pm 5 \pm 5 \text{ MeV}$.

The relatively large (compared to the indirect result) error of the direct measurement of Γ_{inv} reflects the small statistical sample of $e^+e^- \rightarrow \gamma\nu\bar{\nu}$ events available at LEP. Therefore, a significant improvement can be expected from a high-luminosity linear collider running around the Z-boson mass. At such a ‘‘Giga-Z’’ machine, it is envisaged that within 100 days of running, a sample of 10^9 Z-boson decays can be collected [15].

Assuming 50 fb^{-1} of e^+e^- data collected around the Z-boson mass, we examine how this would improve the measurement of the invisible Z width. We are mostly interested in the result that could be obtained by looking for $\gamma + \text{missing energy}$, but will first briefly present the improvement that can be expected for determining the invisible Z width indirectly, as discussed in the previous subsection. We assume [16,17] that the total Z width can be measured a factor of roughly two times more precisely, $\delta\Gamma_{\text{tot}} = \pm 1 \text{ MeV}$, while R_ℓ (assuming universality) and σ_h^0 will be measured with uncertainties $\delta(R_\ell) = \pm 0.018$ and $\delta(\sigma_h^0) = \pm 0.03 \text{ nb}$ (most conservative scenario), or $\delta(R_\ell) = \pm 0.004$ and $\delta(\sigma_h^0) = \pm 0.015 \text{ nb}$ (most optimistic scenario). We refer readers to [16,17] for more details. Further assuming that the correlation matrix between the observables is identical to the one obtained for the combined LEP results,² we estimate that the invisible Z width can be measured with an uncertainty $\delta(\Gamma_{\text{inv}}) = \pm 1.1 \text{ MeV}$ (most conservative) or $\delta(\Gamma_{\text{inv}}) = \pm 0.5 \text{ MeV}$ (most optimistic). For the most optimistic case, the experimental error would be slightly better than the current theoretical error for computing the invisible Z width within the SM, Eq. (2.3). Compared with the current LEP precision, Eq. (2.2), we therefore expect between a factor 1.3

²It is likely that this correlation matrix will be different for the Giga-Z data. As the correlations depend on the details of the analyses, it is not possible for us to predict them at this time. Nonetheless, our estimates of the uncertainties which can be obtained at a linear collider should be trustworthy.

and a factor 3 reduction of the error on Γ_{inv} from the Giga-Z experiment.

For illustrative purposes, if one assumes that the results for Γ_{inv} and $\Gamma_{\ell\ell}$ at the Giga-Z agree with the central values obtained at LEP, one would measure $(\Gamma_{\text{inv}}/\Gamma_{\ell\ell})^{\text{Giga-Z}} = 5.942 \pm 0.012$ (most conservative) or $(\Gamma_{\text{inv}}/\Gamma_{\ell\ell})^{\text{Giga-Z}} = 5.942 \pm 0.006$ (most optimistic). Translating into a “number of neutrinos” we would have

$$N_{\nu}^{\text{Giga-Z}} = 2.984 \pm 0.006 \quad (\text{most conservative}), \quad (2.9)$$

$$N_{\nu}^{\text{Giga-Z}} = 2.984 \pm 0.003 \quad (\text{most optimistic}), \quad (2.10)$$

either 2.5σ or 5σ away from the SM prediction. In the most optimistic case, the experimental error would start to approach the theoretical error which goes into computing the

neutrino to charged-lepton partial decay width ratio.³ Therefore, given the assumptions outlined above, the weak 2σ effect observed at LEP could grow to something between a 3σ evidence and a 5σ discovery that something is “wrong” (assuming that this discrepancy is genuine and not just a statistical fluctuation).

A much more significant improvement can be anticipated for the direct measurement of the invisible Z width. In order to compute the precision to which it can be directly measured at the Giga-Z experiment, we calculate the cross section for $e^+e^- \rightarrow \gamma + \text{invisible}$ for different center-of-mass energies. We require the photon energy to be above $E_{\gamma}^{\text{min}} = 1$ GeV, and that it is emitted at an angle with respect to the beam axis larger than $\theta_{\gamma}^{\text{min}} = 20^\circ$. For any set of cuts on the photon energy and emission angle, the SM cross section for $\nu\bar{\nu}\gamma$ is given by [18]

$$\sigma_{\nu\bar{\nu}\gamma} = \int_{x_{\text{min}}}^1 dx \int_{-\cos\theta_{\gamma}^{\text{min}}}^{\cos\theta_{\gamma}^{\text{min}}} dy \frac{\alpha G_F^2 m_W^4}{48\pi^2} \frac{sx(1-x)}{\kappa_+ \kappa_-} [\eta_+^2 F(\eta_+) + \eta_-^2 F(\eta_-)], \quad (2.11)$$

where

$$F(\eta) = \frac{N_{\nu}(g_v^2 + g_a^2) + 3(g_v + g_a) \left(1 - \frac{s(1-x)}{m_Z^2} \right) \frac{1}{\eta} \left[3 + \frac{2}{\eta} - 2 \left(1 + \frac{1}{\eta} \right)^2 \log(1 + \eta) \right]}{\left(1 - \frac{s(1-x)}{m_Z^2} \right)^2 + \frac{\Gamma_{\text{tot}}^2}{m_Z^2}} + \frac{6}{\eta} \left[(1 + \eta) \left(1 - \frac{2}{\eta} \log(1 + \eta) \right) + 1 \right], \quad (2.12)$$

$$\eta_{\pm} = \frac{s - \kappa_{\pm}}{m_W^2}, \quad (2.13)$$

$$\kappa_{\pm} = \frac{s}{2} x(1 \pm y). \quad (2.14)$$

$\sqrt{s} = 2E_{\text{beam}}$, E_{beam} is the beam energy, $x = E_{\gamma}/E_{\text{beam}}$, $x^{\text{min}} = E_{\gamma}^{\text{min}}/E_{\text{beam}}$, $y = \cos\theta_{\gamma}$ is the angle of the photon with respect to the beam direction, $g_v = -1/2 + 2\sin^2\theta_W$ and $g_a = -1/2$ are the SM vector and axial-vector $Ze\bar{e}$ couplings. We have assumed that the charged-current $We\bar{\nu}$ coupling and the neutral current $Z\nu\bar{\nu}$ couplings are all equal to their SM values. We will revisit some of these hypotheses in the next section. The following approximation is made when deriving Eq. (2.11): the contribution from the third diagram in Fig. 1, suppressed by an extra W -boson propagator, is neglected, along with the finite width of the W boson (a good approximation for “space-like” W boson exchange).

The main SM physics backgrounds come from the processes $e^+e^- \rightarrow e^+e^-\gamma(n\gamma)$, $e^+e^- \rightarrow \mu^+\mu^-\gamma(n\gamma)$, $e^+e^- \rightarrow \tau^+\tau^-\gamma(n\gamma)$, $e^+e^- \rightarrow \gamma\gamma\gamma(n\gamma)$ and $e^+e^- \rightarrow l^+l^-\nu\bar{\nu}\gamma$ (see, for example, [12]). They are characterized by a trans-

verse tagging photon with $E_{\gamma} > 1$ GeV and additional high-energy charged particles and/or photons which are lost in the “blind” regions of the detector located around the beam pipe. The expected contributions from the process $e^+e^- \rightarrow \nu\bar{\nu}\nu\bar{\nu}\gamma(\gamma)$ are negligible and will not be considered henceforth. We have computed these background cross sections using Monte Carlo integration methods. The number of background events can be reduced by vetoing on additional energy deposits in the calorimeters, in particular at low angles. As a concrete example, we consider the TESLA detector concept [19], which envisions a luminosity calorimeter

³This theoretical error, however, is currently dominated by the uncertainty on the top-quark mass and the uncertainty on the Higgs boson mass. It is likely that by the time a Giga-Z experiment takes data, these two quantities will be much better known.

TABLE I. Cross section for $e^+e^- \rightarrow \nu\bar{\nu}\gamma$ (signal) at a linear collider for three center-of-mass energies around the Z-boson mass. Also tabulated is the expected number of signal events, S , assuming that 50 fb^{-1} of data are collected with an efficiency of 65%. See text for details. Finally, in the last column we compute $1/\sqrt{S}$, the statistical error which one expects to obtain when extracting the signal.

\sqrt{s}	$\sigma(\nu\bar{\nu}\gamma)$	$S(\nu\bar{\nu}\gamma)$	$1/\sqrt{S}$
$m_Z = 91.1875 \text{ GeV}$	53.5 pb	1.74×10^6	0.076%
$m_Z - 1 \text{ GeV}$	28.6 pb	0.93×10^6	0.10%
$m_Z + 1 \text{ GeV}$	109 pb	3.5×10^6	0.053%

(LCAL) at very small angles ($4.6 < \theta < 27.5 \text{ mrad}$). Together with the low-angle tagger (LAT) at $27.5 < \theta < 83 \text{ mrad}$, the LCAL provides an excellent angular coverage for the background veto. In fact, we estimate that the cross sections for all background sources mentioned above are reduced to a negligible level of $\sim 0.1 \text{ fb}$.

A more detailed background analysis would require the inclusion of detector effects. For example, additional contributions arise from the processes $e^+e^- \rightarrow \nu\bar{\nu}X$ and $e^+e^- \rightarrow e^+e^-X$ with $X = \pi^0, \eta, \eta', f_2(1270)$ where the neutral hadron is misidentified as a photon. However, while the contribution from the $\nu\bar{\nu}X$ cross section is expected to be very small because of phase-space constraints, the two-photon production of resonances in $e^+e^- \rightarrow e^+e^-X$ can be reduced to a negligible level using the low-angle veto as discussed above. Since the total background level is very small, additional detector effects should therefore play a minor role. In Table I, we quote the results obtained for the signal cross section, for different center-of-mass energies, including leading-log initial-state radiation and beamstrahlung using the program CIRCE [20]. Also given are the expected number of events which are to be recorded after accumulating

50 fb^{-1} of data in a Giga-Z experiment, assuming 65% selection efficiency⁴ in the given kinematic region. We also compute the figure of merit $1/\sqrt{S}$ for the different center-of-mass energies. Given that the background cross section is well below 1 pb, we expect the number of background events to be negligible. The figure of merit is the relative statistical uncertainty for measuring the invisible Z width. For a 50 fb^{-1} Giga-Z experiment, one can expect statistical errors around the 0.1% level, about a factor 25 improvement over the statistical error quoted by L3.

Systematic uncertainties may dominate the very small statistical errors estimated above. In order to correctly estimate the systematic uncertainties, one should perform a complete detector simulation, which is clearly beyond the intentions of this paper. Instead, we analyze the systematic errors that were computed by the LEP experiments for the same measurement, and extrapolate them for a TESLA-like Giga-Z experiment. We concentrate mostly on the L3 1998 systematic error computations, obtained from the analysis of 100 pb^{-1} of data [10]. These are presented in Table II. For illustrative purposes, we also quote the systematic errors computed in earlier analyses by ALEPH (which analyzed 19 pb^{-1} of data [11]) and OPAL (based on 40.5 pb^{-1} of data [12]). We make use of these results to verify that our estimates are reasonable.

Most of the systematic uncertainties go down simply because the number of events goes up. The same trend is observed when one compares the L3 result with the older results from the other LEP experiments. This can be appreciated, for example, by looking at columns 2 and 3 in Table II.

⁴This is the selection efficiency obtained in the OPAL analysis [12]. It is slightly better than the one obtained by the L3 experiment [10].

TABLE II. Systematic uncertainties for measuring the invisible Z width, in percent and (inside the square brackets) expressed as $\delta\Gamma_{\text{inv}}$. The source of the systematic uncertainty is listed in the first column (see text for details) while the second through fourth columns contain the estimates obtained by ALEPH [11] in 1993 (19 pb^{-1} of data), OPAL [12] 1995 (40.5 pb^{-1} of data) and L3 [10] 1998 (100 pb^{-1} of data). Our projection for TESLA running in the Giga-Z mode (50 fb^{-1}) is presented in the last column. N/C indicates that this source of systematic error was not considered or not quoted in the specific published result.

Source of Systematic Error	ALEPH 93	OPAL 95	L3 98	TESLA (estimate)
event generator for $\nu\bar{\nu}\gamma$	1% [5 MeV]	1.2% [6 MeV]	0.7% [3.5 MeV]	0.1% [0.5 MeV]
event generator for $e^+e^- \gamma$	1% [5 MeV]	in bkgd. subtr.	0.7% [3.5 MeV]	0.1% [0.5 MeV]
energy calibration	1.5% [7.5 MeV]	1.7% [9 MeV]	0.8% [4 MeV]	0.03% [0.15 MeV]
luminosity	0.6% [3 MeV]	0.6% [3 MeV]	0.37% [1.8 MeV]	0.06% [0.3 MeV]
fit procedure	N/C	0.9% [5 MeV]	0.5% [2.5 MeV]	0.1% [0.5 MeV]
selection efficiency and veto efficiency	3.9% [18 MeV]	1.7% [9 MeV]	0.8% [4 MeV]	<0.08% [0.4 MeV]
trigger efficiency	1.8% [9 MeV]	0.5% [2.5 MeV]		
background subtraction	0.2% [1 MeV]	0.1% [0.5 MeV]	1% [4.8 MeV]	0.01% or 0.04% [(0.05 or 0.21) MeV]
cosmic ray background	N/C	1.6% [8 MeV]	1.7% [8.4 MeV]	negligible
random vetoing (occupancy)	N/C	in bkgd. subtr.	0.25% [1.7 MeV]	negligible
	0.5% [2.5 MeV]	0.5% [2.5 MeV]	N/C	negligible
total error (added in quadrature)	6.8% [34 MeV]	3.3% [17 MeV]	2.5% [12.3 MeV]	0.20% [1 MeV]

(i) By “event generators” we refer to the numerical accuracy of the computation of the signal and the background given a set of kinematical constraints. We expect that these theoretical calculations will improve by a factor of roughly 10 by the time a Giga-Z experiment is ready to take data.

(ii) The “energy calibration” of the experiment is crucial for measuring the photon energy and hence the lower bound E_γ^{\min} defined above. The improvement suggested in the table can be achieved by calibrating the photon energy via a comparison of other processes that yield a photon, such as $e^+e^- \rightarrow \ell^+\ell^-\gamma$, $e^+e^- \rightarrow X\pi^0 \rightarrow X\gamma\gamma$, etc. The calibration error will decrease with an increase in the statistical sample (i.e., proportional to $1/\sqrt{N}$). Since we expect 500 times more events at the Giga-Z experiment compared to LEP, the error should improve by a factor $\sqrt{500} \approx 22$.

(iii) The luminosity is obtained through the measurement of Bhabha scattering. Given that the cross section for Bhabha scattering around the Z -boson mass is $\sigma_{\text{Bhabha}} \approx 50$ nb, one expects a tiny statistical error on the luminosity measurement of $\delta_{\text{lum}}^{\text{stat}} \approx \pm 0.0025\%$. The systematic error constrained by luminosity monitoring has been studied for the TESLA proposal by [17], and is given by $\delta_{\text{lum}}^{\text{sys}} = \pm 0.03\% \pm 0.05\%$, where the first number is related to experimental systematic effects, while the second one to theoretical effects, including beamstrahlung, etc. Combining the three errors in quadrature, one obtains $\delta_{\text{lum}} \approx \pm 0.06\%$.

(iv) By “fit procedure” we mean the error which comes from the uncertainties of other input physics parameters needed in order to extract the invisible Z width and estimate the background level. These include m_Z , Γ_{tot} , and Γ_{ee} . Using the latest combined results from LEP, we expect a factor of 5 improvement with respect to the L3 analysis, while the Giga-Z data should provide an extra factor of 2 improvement on Γ_{ee} .

(v) The “selection and veto efficiencies” are estimated via a comparison of data and Monte Carlo simulations. The uncertainty is partially controlled by the size of the data sample, so again we can expect a factor $\sqrt{500} \approx 22$ improvement of both of these systematic uncertainties. The other contribution to the uncertainty comes from the quality of the Monte Carlo simulations, which we assume will improve by roughly a factor of 10.

(vi) The “trigger efficiency” can be studied via control samples with independent triggers (e.g. hadronic events, $\ell^+\ell^-\gamma$, etc.), indicating that the systematic error is also related to the overall data sample. We note that the L3 estimate presented in the fourth column of Table II is much larger than the ALEPH or OPAL numbers presented in the second and third column. We therefore quote two estimates for the trigger efficiency, one based on the L3 estimate and one on the ALEPH estimate.

(vii) After applying selection and kinematic cuts, some background contribution remains, and it needs to be subtracted. The precise value of the remaining background crucially depends on the performance of the detector in rejecting charged particles at small angles. The understanding of the detector systematics in this region is afflicted with some systematic uncertainty. We conservatively attribute an error of

20% to the computation of the background contamination. Note, however, that since background levels can be reduced to negligible levels in the presence of a luminosity calorimeter, the impact of this uncertainty is negligible.

(viii) The much higher luminosity of a Giga-Z machine should render cosmic rays irrelevant. The impact of detector and beam-related noise can be estimated with special “zero-bias” triggers, with negligible uncertainty.

In summary, we estimate the combined systematic error to be around $(\delta\Gamma_{\text{inv}})^{\text{sys}} \approx \pm 1$ MeV. Due to the disparity among different LEP measurements, we can, in principle, quote a “best” and “worst” case scenario. In the best case, the trigger efficiency is $\pm 0.01\%$ uncertain, while in the worst case, the trigger efficiency is measured with a $\pm 0.05\%$ error. In practice, however, the “best” and “worst” cases yield the same total systematic error. Note that all uncertainties have been added in quadrature.

Our estimate of the total systematic error is already a factor of two larger than the statistical error estimated earlier, $(\delta\Gamma_{\text{inv}})^{\text{stat}} \approx \pm 0.5$ MeV, so the question of whether the accumulation of many more events would lead to a significant improvement of the measurement requires a more detailed analysis. The overall error, $\delta\Gamma_{\text{inv}} \approx \pm 1.3$ MeV, is slightly smaller than the one obtained at LEP via the indirect method, Eq. (2.2), and is comparable to the estimated indirect result that might be obtained by the Giga-Z experiment itself [$\delta(\Gamma_{\text{inv}}) = \pm (0.5 \text{ to } 1.1)$ MeV]. More importantly, the direct measurement at the Giga-Z experiment is expected to be a factor 15 times more precise than the current direct measurement obtained by the four LEP collaborations and a factor of roughly 6 times more precise than the ultimate precision that can be reached by analyzing the entire LEP data set. Finally, a combined result (if one could be properly defined) would have an error bar that is similar to the current theoretical uncertainty in calculating the partial width for $Z \rightarrow \nu\bar{\nu}$ in the SM.

III. $Z\nu\bar{\nu}$ COUPLINGS AWAY FROM THE Z POLE

At any center-of-mass energy, the differential cross section for $e^+e^- \rightarrow \gamma\nu\bar{\nu}$, in the SM, assuming generic $Z\nu\bar{\nu}$ couplings and neglecting neutrino-mass effects is given by

$$\frac{d\sigma_{\gamma\nu\bar{\nu}}}{dx} = \left(\sum_{\alpha=e,\mu,\tau} [(g_L^{\nu\alpha})^2 + (g_R^{\nu\alpha})^2] ZZ(s,x) \right) + (g_L^{\nu e}) WZ(s,x) + WW(s,x). \quad (3.1)$$

The leading order Feynman diagrams are shown in Fig. 1. Here x and s are defined as in Eq. (2.11), while ZZ , WW , and ZW are functions of s,x (plus several standard model parameters, including m_Z^2 , Γ_{tot} , and the Zee couplings). The first term corresponds to the square of the s -channel Z -boson exchange amplitude and the third term to the square of the t -channel W -boson exchange amplitude, while the second term arises from the interference between these two contributions. We have made explicit the dependency on the $Z\nu_\alpha\bar{\nu}_\alpha$ left-handed and right-handed couplings (α

$=e, \mu, \tau$). In the SM, $g_L^{\nu_e} = g_L^{\nu_\mu} = g_L^{\nu_\tau} = 1/2$, while $g_R^{\nu_e} = g_R^{\nu_\mu} = g_R^{\nu_\tau} = 0$. We assume throughout that the charged-current $W\ell\bar{\nu}_e$ coupling agrees with its SM prediction. Experimentally, the charged-current neutrino-electron coupling is well constrained to be purely left-handed (at the few percent level), and its value is accurately determined. Needless to say, the $W\ell\bar{\nu}$ couplings are much better constrained (directly) than the $Z\nu\bar{\nu}$ couplings. The most stringent constraints on the nature and value of the $W\ell\bar{\nu}$ couplings are provided by studying weak decays of neutrons, nuclei, muons, and charged pions. We refer readers to, for example, [2,21] for details. As pointed out before, the contribution of the third diagram in Fig. 1 is negligible within the SM, with an impact of less than 0.1% on the total cross section for energies $\sqrt{s} < 200$ GeV. This statement remains true even when considering possible anomalous γWW couplings, since their effect is constrained by LEP II data to be less than about 15% of the SM contribution [4].

At an e^+e^- collider it is impossible to distinguish $\nu_\tau\bar{\nu}_\tau$ from $\nu_\mu\bar{\nu}_\mu$ final states, which allows one to rewrite the coefficient of ZZ in Eq. (3.1) as

$$\sum_{\alpha=e,\mu,\tau} [(g_L^{\nu_\alpha})^2 + (g_R^{\nu_\alpha})^2] \equiv N_\nu [(g_L^{\nu_e})^2 + (g_R^{\nu_e})^2], \quad (3.2)$$

where N_ν is the effective neutrino number. This definition of N_ν only agrees with the one in Eq. (2.4) if the charged-lepton couplings to the Z boson are fixed to their SM values. As a matter of fact, the right-handed $Z\nu\bar{\nu}$ coupling g_R can be more generally interpreted as coupling of the Z boson to other exotic, invisible final states. We will return to this point in Sec. IV.

In order to analyze the kinematics of $e^+e^- \rightarrow \gamma\nu\bar{\nu}$, it proves useful to utilize the ‘‘missing mass,’’ defined to be the mass of the system recoiling against the photon: $M_{\nu\bar{\nu}} \equiv \sqrt{s(1-x)}$. If there are no additional photons, this coincides with the $\nu\bar{\nu}$ invariant mass. For missing mass close to the Z-boson mass, the cross section for $e^+e^- \rightarrow \gamma\nu\bar{\nu}$ is dominated by the ZZ term, and one can only, in practice, measure $N_\nu(g_L^2 + g_R^2)$.⁵ On the other hand, for a range of values of the missing mass above the Z-boson mass (or the photon energy, $E_\gamma = xE_{\text{beam}}$, below the Z-boson mass), the ZZ, WZ and WW contributions are comparable and one is, in principle, sensitive to both g_L and $N_\nu(g_L^2 + g_R^2)$. For very high values of $M_{\nu\bar{\nu}}$, however, the WW-term dominates, and one loses sensitivity to both $N_\nu(g_L^2 + g_R^2)$ and g_L . Figure 2 depicts $d\sigma_{\gamma\nu\bar{\nu}}/dM_{\nu\bar{\nu}}$ as a function of $M_{\nu\bar{\nu}}$, for $\sqrt{s} = 170$ GeV, $N_\nu = 3$ and the SM values for the neutral-current neutrino couplings. Figure 2 also displays the different contributions to the differential cross section. As one can easily note, for $M_{\nu\bar{\nu}}$ around the Z-boson mass the differential cross section is completely dominated by the ZZ term, while at the largest values of $M_{\nu\bar{\nu}}$ the WW piece dominates. The interference WZ

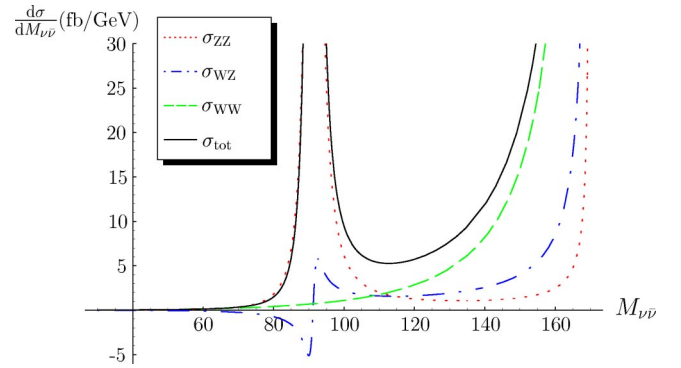


FIG. 2. The differential cross section for $e^+e^- \rightarrow \gamma\nu\bar{\nu}$ as a function of the invariant mass of the $\nu\bar{\nu}$ system, $M_{\nu\bar{\nu}}$, for $\sqrt{s} = 170$ GeV, assuming SM values for the number of neutrino species and the neutrino neutral-current couplings. We also show the different contributions to the differential cross section (ZZ, WZ, and WW—see text for details). The sharp increase of the differential cross section as $M_{\nu\bar{\nu}}$ approaches \sqrt{s} is due to an infrared singularity at vanishing photon energy.

term, which changes sign at the Z-boson mass, becomes comparable to the other two contributions at $M_{\nu\bar{\nu}} \sim 100$ GeV. For a fixed value of N_ν , one can therefore measure g_L directly by measuring the cross section for $e^+e^- \rightarrow \gamma\nu\bar{\nu}$ above $M_{\nu\bar{\nu}} \sim 100$ GeV. Before pursuing this further, however, we will first review what is currently known about the values of g_L and g_R .

A. Current knowledge of the g_L^{ν} and g_R^{ν} couplings to the Z boson

The currently most precise value of $N_\nu(g_L^2 + g_R^2)$ can be extracted from the indirect measurement of the invisible Z width, Eq. (2.2). For $N_\nu = 3$, the region of the $g_L \times g_R$ plane allowed by Eq. (2.2) is characterized by a ring. Figure 3 (left) shows the current LEP constraint at one and two sigma confidence levels (the two contours are indistinguishable in the figure).

More information is provided by $\nu-e$ elastic scattering experiments. The CHARM II experiment at CERN collected a large sample of $\nu_\mu e \rightarrow \nu_\mu e$ and $\bar{\nu}_\mu e \rightarrow \bar{\nu}_\mu e$ events [22]. By using information on the Zee vector and axial vector couplings [23] measured very accurately at LEP and SLC (see, for example, [1,3,4] and references therein), CHARM II is capable of measuring $|g_L^{\nu\mu}|$ rather well:

$$|g_L^{\nu\mu}| = 0.502 \pm 0.017 \quad (\text{CHARM II}), \quad (3.3)$$

where we quote the updated number presented by the PDG [2]. Furthermore, CHARM II can also measure $|g_L^{\nu e}|$ (CHARM II) = 0.528 ± 0.085 via a small ‘‘contamination’’ of $\nu_e(\bar{\nu}_e)e \rightarrow \bar{\nu}_e(\bar{\nu}_e)e$ events which are present in its data set. This result agrees with the one obtained in a $\nu_e - e$ elastic scattering experiment at the Los Alamos Meson Physics Facility (LAMPF): $|g_L^{\nu e}|$ (LAMPF) = 0.46 ± 0.14 [24]. In order to claim that these neutrino-electron scattering

⁵Henceforth, we replace $g_{L,R}^{\nu_e}$ with $g_{L,R}$.

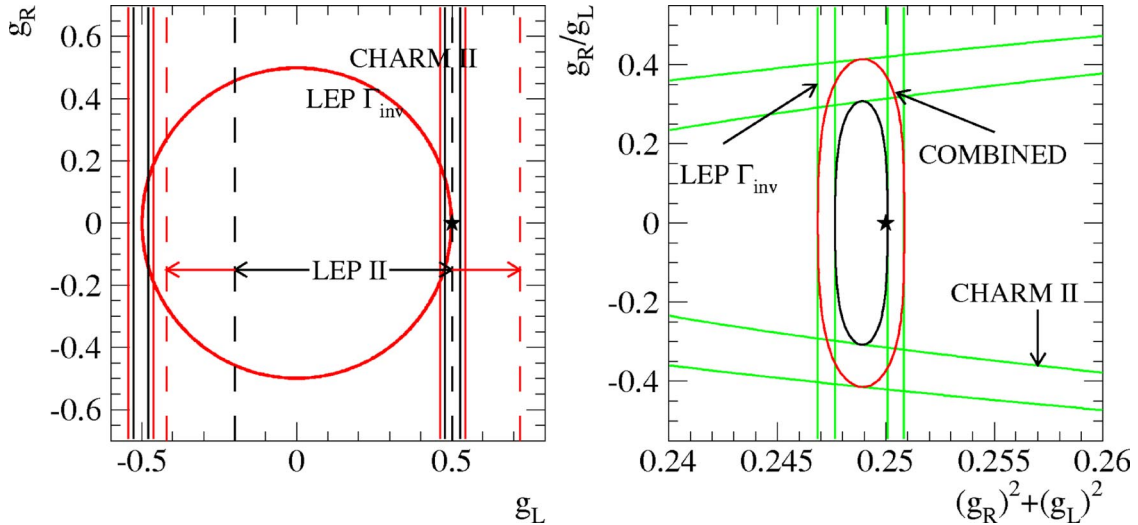


FIG. 3. (Left) Current constraint (one and two sigma confidence level contours) on g_L and g_R from the LEP (indirect) measurement of the invisible Z width and the CHARM II experiment, on the $g_L \times g_R$ plane. The SM expectation is indicated by a star. We have assumed $N_\nu=3$ for the LEP result, and $g_L = g_L^{\nu\mu}$ for the CHARM II result in order to have both experiments constrain the same physical parameters. We also include the current constraint on g_L that can be obtained from published LEP II data, also at the one and two sigma confidence level. See text for details. (Right) The one and two sigma allowed regions which are selected by combining the LEP and CHARM II results. The individual LEP and CHARM II constraints (at one and two sigma confidence levels) are also depicted. Note that one is unable to distinguish $g_L > 0$ from $g_L < 0$.

experiments are indeed sensitive only to the left-handed $Z\nu\bar{\nu}$ couplings, we are assuming that the charged-current interactions responsible for producing the neutrino beam are purely left-handed and neutrino-mass effects can be neglected. The region of the $g_L \times g_R$ plane allowed by Eq. (3.3) is depicted as vertical bars (at one and two sigma confidence level) in Fig. 3 (left). The SM value for $(g_L, g_R)_{SM}$ is represented by a star.

In order to combine the LEP invisible Z -width constraint with the CHARM II bound, it is useful to display the result on the $(g_L^2 + g_R^2) \times g_R/g_L$ plane. In this case, the region depicted in Fig. 3 (right) is selected at one and two sigma confidence level. Here, the region allowed by the invisible Z -width measurement at LEP is characterized by vertical bars, while the CHARM II bound is characterized by a “parabolic” region. It is important to emphasize that in order for this joint analysis to make sense, we are assuming that the $Z\nu\bar{\nu}$ couplings are universal (the same for all three neutrino flavors), that there are three neutrino species (coupling to the Z boson), and that there are no extra contributions to invisible Z -boson decays or electron-neutrino scattering. The result obtained is rather good: $|g_L|$ has been measured with relatively good precision ($0.45 \leq |g_L| \leq 0.5$). On the other hand, $|g_R|$ is only mildly bounded from above ($|g_R| \leq 0.2$), and we have no information concerning the sign of g_L .

The NuTeV experiment also provides a measurement of the muon-neutrino coupling to the Z boson. Assuming the value of $\sin^2\theta_W$ obtained at other experiments, SM values for the $Zq\bar{q}$ couplings, and fixing the $W\mu\bar{\nu}_\mu$ coupling to its SM value, one can interpret the NuTeV result as a measurement of $|g_L^{\nu\mu}|$. From [7],

$$|g_L^{\nu\mu}| = 0.4971 \pm 0.0011 \quad (\text{NuTeV}). \quad (3.4)$$

This result is 15 times more precise than the CHARM II result [Eq. (3.3)], and 1.4 times more precise than the LEP result [Eq. (2.2)]. Furthermore, while its central value is roughly 3σ away from the SM prediction, Eq. (3.4) is perfectly (within one sigma) consistent with Eq. (2.2), which also differs from the SM prediction by 1.5σ , and Eq. (3.3), which is a lot less precise. Nonetheless, we choose not to include the NuTeV result in our studies, for a few reasons. Many assumptions have to be made before one can interpret the NuTeV result as a measurement of the $Z\nu\bar{\nu}$ coupling, including the assumption that the Z -boson coupling to quarks is as prescribed by the SM. In the case of the CHARM II result, in contrast, we only had to input the values of g_ν and g_a which were directly measured at LEP. More importantly, there is a significant amount of discussion in the literature concerning whether nuclear and/or hadronic effects might further modify the NuTeV result (see, for example, [9]) and it is still premature to compare Eq. (3.4) with the other measurements of the $Z\nu\bar{\nu}$ couplings discussed earlier.

We return now to Eq. (3.1) and investigate the impact of the LEP II data. These were collected at different center-of-mass energies above the Z -boson mass, but not all of them have been used to measure the cross sections for $e^+e^- \rightarrow \gamma\nu\bar{\nu}$. A useful summary is given in Ref. [25]. In order to extract g_L , we compute the total cross section at each \sqrt{s} imposing the various fiducial and kinematic cuts of each measurement. The coefficient for the ZZ term in Eq. (3.1) is constrained to the value obtained from Γ_{inv}^{LEP} , Eq. (2.2). We construct an overall χ^2 function, taking all systematic uncertainties to be wholly correlated. Since the measurement er-

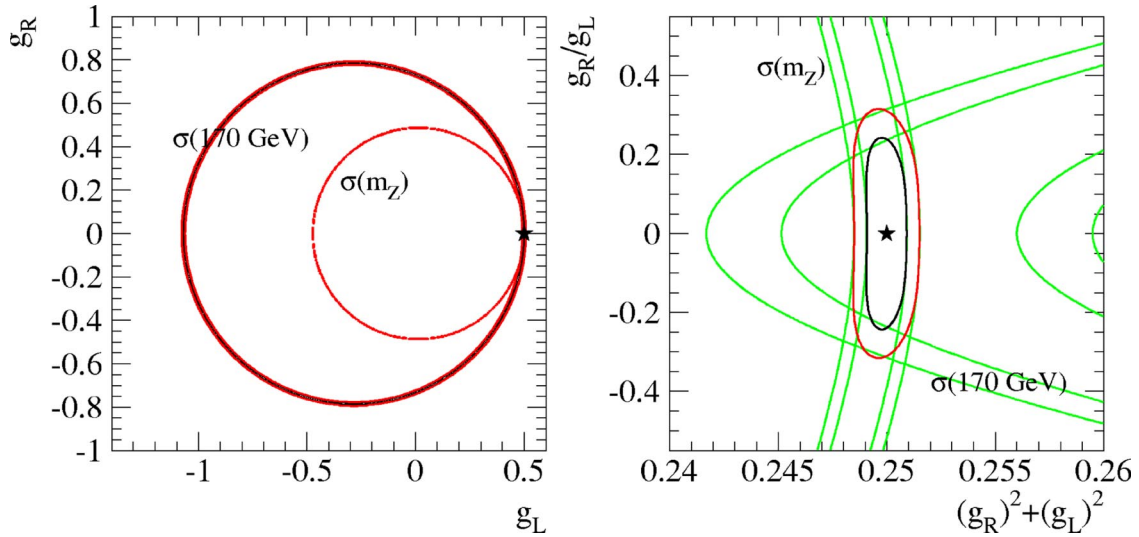


FIG. 4. (Left) Projected constraint (one and two sigma confidence level contours) on g_L and g_R from $e^+e^- \rightarrow \gamma\nu\bar{\nu}$ at a linear collider assuming 50 fb^{-1} of data are collected at the Z-boson mass [$\sigma(m_Z)$] and at $\sqrt{s}=170 \text{ GeV}$ [$\sigma(170 \text{ GeV})$], on the $g_L \times g_R$ plane. For the result obtained at $\sqrt{s}=170 \text{ GeV}$, we impose a constraint on the invariant mass of the $\nu\bar{\nu}$ system ($M_{\nu\bar{\nu}} > 100 \text{ GeV}$) in order to remove the radiative return to the Z-boson mass. (Right) The one and two sigma allowed regions which are selected by combining the results obtained at the two different center of mass energies in the $(g_R^2 + g_L^2) \times g_R/g_L$ plane. The individual constraints obtained at the two distinct center-of-mass energies are also depicted. In both figures, the SM expectation is indicated by a star and we have assumed $N_\nu=3$.

rors are dominated by the statistical uncertainties, the correlations are not very important numerically. Minimization of χ^2 gives

$$g_L = 0.16 \pm 0.23 \quad (\text{LEP II}), \quad (3.5)$$

and $\chi^2=9.6$ for 23 degrees of freedom. The allowed range of g_L is indicated in Fig. 3 (left) at the one and two sigma confidence levels.⁶ These data do eliminate the region $g_L \approx -\frac{1}{2}$, otherwise allowed by the CHARM II and LEP I data, at a little more than the two sigma confidence level.

The LEP II data could provide a much stronger constraint. First of all, only ALEPH has published measurements from its entire data sample. If the other collaborations completed the analysis of all data with $\sqrt{s} > 160 \text{ GeV}$ using the fiducial and kinematic cuts of the published measurements, we estimate that the one-parameter error on g_L would decrease to $\delta(g_L) = 0.15$. More importantly, the published LEP II analyses are not optimized for measuring g_L . As is apparent from Fig. 2, events with a missing mass close to the Z-pole mass will dominate the total cross section and dilute the impact of the interference term, WZ. We estimate that the imposition of a lower limit on the missing mass should improve the sensitivity to g_L by about a factor of three. The optimal value for this cut is around 95–100 GeV. If all LEP II data were analyzed with this cut imposed, the total error on g_L should decrease to $\delta(g_L) = 0.05$ —better than a factor four improvement. Of course, the central value in Eq. (3.5) is also likely

to change. Only an analysis of the actual data taken by the LEP collaborations will reveal it.

B. Measuring g_L' and g_R' in a linear collider

We now discuss how a linear collider can improve on the existing results discussed above. In order to do this we compute the $e^+e^- \rightarrow \gamma\nu\bar{\nu}$ cross section at a linear collider at $\sqrt{s}=m_Z$ and $\sqrt{s}=170 \text{ GeV}$. The latter collider center-of-mass energy can also be used, for example, for precisely measuring the W-boson mass [26].⁷ Assuming that the central value for Γ_{inv} obtained at the Giga-Z machine agrees with the SM prediction, we can translate an expected $\pm 0.25\%$ uncertainty, as estimated in Sec. II, into an allowed region of the $g_L \times g_R$ plane. This region is characterized by a ring approximately centered around the origin, and is depicted in Fig. 4 (left). The shape and width of the curve are almost identical to the one depicted in Fig. 3 (left) for the LEP indirect measurement of the invisible Z width. Upon closer inspection, one should be able to see that the center of the ring is slightly shifted to the right. This small effect is due to the nonzero contribution of the W-boson exchange diagram. Furthermore, the precision obtained from the direct measurement of the invisible Z width at Giga-Z is only slightly better than the current indirect LEP result, and slightly worse than the future indirect result that might be obtained by Giga-Z (see Sec. II). However, it is interesting to discuss with what precision the neutrino neutral-current couplings can be measured at a linear collider when one com-

⁶In order to facilitate comparison with the other measurements, the error on g_L has been rescaled to correspond to two free parameters.

⁷For our purposes, the choice of the “high” center-of-mass energy is not crucial. Any value in the range [150–200] GeV will yield similar results.

TABLE III. Systematic uncertainties for measuring the cross section for $e^+e^- \rightarrow \gamma\nu\bar{\nu}$ at center-of-mass energies above ~ 160 GeV, in percentage. The source of the systematic uncertainty is listed in the first column (see text for details) while the second and third columns contain the estimates obtained by OPAL [27] (177 pb^{-1} of data) and ALEPH [28] (628 pb^{-1} of data). Our projection for TESLA running at $\sqrt{s} = 170$ GeV (and collecting 50 fb^{-1} of data) is presented in the last column. N/C indicates that this source of systematic error was not considered or not explicitly quoted.

Source of Systematic Error	OPAL (177 pb^{-1})	ALEPH (628 pb^{-1})	TESLA [estimate] (50 fb^{-1})
event generator—theoretical	0.5%	1.5%	0.2%
event generator—statistical	0.2%	0.5%	$< 0.1\%$
energy calibration	0.4%	N/C	0.025%
luminosity	0.2%	0.5%	0.06%
uncertainty from W/Z -boson mass	N/C	N/C	0.25%
selection efficiency	1.5%	0.6%	0.07%
angular acceptance	0.2%	N/C	0.01%
modeling early γ conversion in material near beam-pipe	0.7%	0.3%	0.2%
tracking	0.5%	N/C	0.1%
total error (added in quadrature)	2.1%	1.8%	0.4%

compares the same observable (namely, the cross section for $e^+e^- \rightarrow \gamma + \text{invisible}$) measured at different center-of-mass energies. By doing this, we reduce the number of assumptions that go into extracting g_L and g_R , and potentially minimize experimental “biases” that may affect different observables in different ways.

We compute the $e^+e^- \rightarrow \gamma\nu\bar{\nu}$ cross section using Eq. (2.11) [18]. As before, we require $E_\gamma > 1$ GeV, and $\theta_\gamma > 20^\circ$. In order to enhance the sensitivity to the WZ interference term [see Eq. (3.1)] we also require $M_{\nu\bar{\nu}} > 100$ GeV. Assuming SM values for the $Z\nu\bar{\nu}$ couplings and $N_\nu = 3$, we obtain

$$\sigma_{\gamma\nu\bar{\nu}}(\sqrt{s} = 170 \text{ GeV}, M_{\nu\bar{\nu}} > 100 \text{ GeV}) = 2.97 \text{ pb}. \quad (3.6)$$

Assuming 50 fb^{-1} of linear collider data and an efficiency of 80% [27,28], we expect around 120 000 $e^+e^- \rightarrow \gamma\nu\bar{\nu}$ events with $M_{\nu\bar{\nu}} > 100$ GeV.

The dominant sources of SM physics background have been listed in Sec. II B (see also [27]) and can be dramatically reduced by vetoing on additional high-energy particles, as discussed earlier. Including the LCAL of the TESLA detector design [19] which helps veto hard particles at very low angles, the total cross section for these backgrounds can be reduced to less than 1 fb.

Other important background sources can arise from detector-related effects. As discussed in [27], the dominant background contributions are related to the processes $e^+e^- \rightarrow \nu\bar{\nu}\ell^+\ell^-$ and $e^+e^- \rightarrow e^+e^-\ell^+\ell^-$, which can mimic events where a photon converts into a lepton pair in the material of the detector. We adopt the values quoted in [27] of $(0.010 \pm 0.001) \text{ pb}$ and $(0.007 \pm 0.002) \text{ pb}$, respectively, for the cross sections for the above background processes. In order to accommodate any changes in detector design com-

pared to the OPAL detector [27], we conservatively allow a factor of two uncertainty on these cross sections, resulting in a total background cross section of about 0.03 pb.

Assuming an integrated luminosity of 50 fb^{-1} , the estimated number of background events is $N_{\text{bkg}} = 1500$. Note that this number, which is very conservative, also includes events with $M_{\nu\bar{\nu}} < 100$ GeV, which have been removed when we estimate the number of signal events. Given the values for the cross sections computed above, we estimate (conservatively) that the statistical uncertainty which can be achieved after accumulating 50 fb^{-1} of $e^+e^- \rightarrow \gamma + \text{invisible}$ at $\sqrt{s} = 170$ GeV is $\sqrt{S+B}/S = 0.3\%$.

Given the very small statistical errors estimated above, we must try to evaluate the size of possible systematic uncertainties. Following the strategy outlined in Sec. II B, we analyze the systematic errors that were computed by the different LEP collaborations for the same observable, and extrapolate them for a TESLA-like linear collider. This time, we concentrate on the analyses of 177 pb^{-1} of data collected by OPAL [27] and 628 pb^{-1} of data collected by ALEPH [28]. Their estimates for different systematic uncertainties are presented in Table III, together with our extrapolation for a linear collider experiment accumulating 50 fb^{-1} of data. There are similar analyses by L3 [29] and DELPHI [30], but their discussions of the systematic errors are not as detailed as the previous two.

We now briefly discuss the origin of the different systematic uncertainties, and how our estimates were obtained. Some of the systematic errors are related to the size of the data sample. Whenever this is the case, we expect a factor $\sqrt{50000/177} \approx 17$ ($\sqrt{50000/628} \approx 9$) improvement with respect to the OPAL (ALEPH) estimate.

(i) As before, we expect the theoretical uncertainty (“event generator—theoretical”) to improve by a factor of 10. The statistical errors associated with these computations

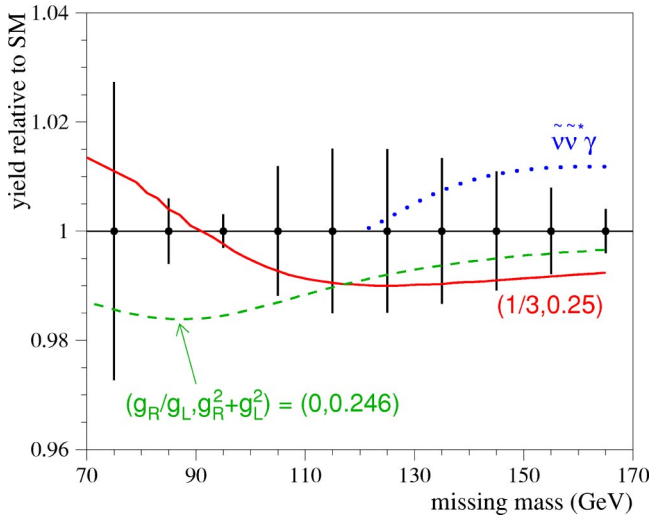


FIG. 5. Comparison of the shape of the missing mass distribution to that expected in the SM. The points with error bars indicate measurement errors for $\sqrt{s} = 170$ GeV and 50 fb^{-1} . The solid curve shows the expected deviation when $g_R/g_L = 1/3$ and $g_R^2 + g_L^2 = 0.25$, while the dashed line shows $g_R = 0$ and $g_R^2 + g_L^2 = 0.246$. (In the SM, $g_R = 0$ and $g_L^2 = 1/4$.) The dotted line shows the contribution from a single species of sneutrinos, with $M_{\tilde{\nu}} = 60$ GeV and no contribution from t -channel chargino exchange.

are only limited by the computer power which is available to perform such numerical calculations, and we expect them to be negligible by the time this experiment takes data.

(ii) As estimated before, the uncertainty related to energy calibration should be controlled by statistics. The same applies for the selection efficiency and the angular acceptance.

(iii) We assume the luminosity uncertainty to be the same as the one estimated in Sec. II B (see [17]). It should be emphasized, however, that the studies performed in [17] concentrated on center-of-mass energies around the Z-boson mass. We are assuming that similar numbers will apply for higher center-of-mass energies.

(iv) There are intrinsic uncertainties in computing the signal and background from the finite accuracy of the input electroweak parameters (of special importance are the values of the W - and Z -boson masses). We assume $\delta(m_Z) = \pm 2$ MeV (from LEP) and $\delta(m_W) = \pm 15$ MeV (from the linear collider itself and the LHC [31]).⁸ This source of systematic uncertainty was not considered in the LEP analyses [27–30]. By taking the combined LEP result for the W -boson mass *at the time of the analysis* [$\delta(m_W) = \pm 0.056$ GeV [32] and $\delta(m_W) = \pm 0.042$ GeV [4]] we obtain a systematic error of 0.9% for the OPAL analysis and 0.7% for the ALEPH analysis, respectively.

(v) Photons can convert to charged particles in the material which surrounds the beam-pipe. This conversion rate is estimated by modeling the material close to the beam-pipe, and depends on the details of the detector layout. A substantial reduction of this error was obtained between the OPAL

[27] and ALEPH [28] analyses, and we assume that at least an extra 50% improvement can be obtained.

(vi) Uncertainties from “tracking” come from knowledge of the performance of the tracking devices near the edges of the fiducial regions. This performance will depend largely on the tracking design and the collider environment near the beam. There will be abundant sources of tagged tracks with which to study tracking, and to define a “good” fiducial region. We assume a factor five improvement over the OPAL uncertainty.

Combining the statistical and systematic errors in quadrature, the total error for the measurement of the $e^+e^- \rightarrow \gamma\nu\bar{\nu}$ cross section at $\sqrt{s} = 170$ GeV is approximately 0.5%. The corresponding allowed region is shown in Fig. 4 (left) in the $g_L \times g_R$ plane, assuming $N_\nu = 3$ and that the measured central value coincides with the SM prediction for (g_L, g_R) , indicated by a star. As expected, the region is characterized by a ring in the $g_L \times g_R$ plane. However, since we have removed the kinematical region dominated by the radiative return to the Z-boson mass, the center of the ring is significantly displaced (to the left) from the origin, while the radius of the ring is significantly larger than the one corresponding to the result obtained around the Z-boson mass (ring centered roughly around the origin). In the case of the SM, the two rings touch at a single point.

The combination of the results obtained at $\sqrt{s} = m_Z$ and $\sqrt{s} = 170$ GeV is shown in the $(g_L^2 + g_R^2) \times g_R/g_L$ plane in Fig. 4 (right). This result is markedly more precise than the LEP+CHARM II result obtained earlier (Fig. 3). We would like to stress that the result depicted in Fig. 3 is *qualitatively* different from the one depicted in Fig. 4. In the former, we are combining very different data (obtained, for example, at very different center-of-mass energies), collected at completely different experiments. Consequently, assumptions are required in order to state that the measurements are sensitive to the same physical parameters. In the latter, we are comparing the same physical observable measured with the same detector, differing only by the center-of-mass energy.

Thus far we have considered only the integrated cross section measured with a few kinematic cuts. The relative contributions to $d\sigma_{\gamma\nu\bar{\nu}}/dM_{\nu\bar{\nu}}$ depicted in Fig. 2 depend on both g_L and g_R . The ZZ term will change if either g_L or g_R varies, while the interference term, WZ , varies only with g_L . The WW term is independent of both g_L and g_R under the assumption that the charged weak interactions are the same as in the SM. Consequently, the shape of the missing mass distribution varies in a nontrivial way as g_L and/or g_R deviate from their SM values. We have estimated the statistical errors for 10 GeV bins in the missing mass, and present the result relative to the SM expectation in Fig. 5. As illustration, we show the expected deviations for two sets of non-SM values for the $Z\nu\bar{\nu}$ couplings, both of which are allowed by current data. In the first case, we take the SM value for $\Gamma_{\nu\bar{\nu}}$ but allow g_R to be one third of g_L . The solid line shows the result: no deviation at the Z-boson pole and a more or less constant reduction in the cross section for $M_{\nu\bar{\nu}} > 105$ GeV. In the second case, we retain $g_R = 0$ as in the SM, but reduce $\Gamma_{\nu\bar{\nu}}$ by less than 2%. As indicated by the dashed line, a large

⁸Some studies suggest that $\delta(m_W) = \pm 6$ MeV could be obtained by scanning around the W^+W^- -production threshold region [26].

deviation is observed at the Z -boson mass, but it nearly disappears for high missing mass, where the WW term dominates. In this sense, a comparison of the bin $M_{\nu\bar{\nu}} \sim 90$ GeV to the bin $M_{\nu\bar{\nu}} \sim 165$ GeV is tantamount to the NuTeV measurement of the $Z\nu\bar{\nu}$ -coupling suppression factor ρ_0 . Experimentally this comparison would be exceptionally clean.

We conclude by commenting on the effect of relaxing the assumption that $N_\nu=3$. If one considers N_ν to be a free parameter during the “data” analysis, no constraint on g_R^2 , as defined in Eq. (3.2), can be obtained, while a “measurement” of g_L , to be performed in a way similar to our measurement of g_L from the LEP II data, can still be performed. This is easy to understand. Because there is no W -boson exchange diagram for the $\nu_{\mu,\tau}\bar{\nu}_{\mu,\tau}$ final states, one could have redefined

$$N_\nu[(g_L^{\nu_e})^2 + (g_R^{\nu_e})^2] \equiv (g_L^{\nu_e})^2 + (g_{\text{others}})^2, \quad (3.7)$$

where $g_{\text{others}} \equiv (N_\nu - 1)(g_L^{\nu_e})^2 + N_\nu(g_R^{\nu_e})^2$. It is easy to see that, via $e^+e^- \rightarrow \gamma +$ invisible one is only sensitive to $g_L^{\nu_e}$ and $(g_{\text{others}})^2$, independent of whether g_{others} is the Z -boson coupling to the SM $\nu_{\mu,\tau}$, right-handed neutrinos, or other exotic invisible final states.

IV. NEW PHYSICS CONTRIBUTIONS TO THE INVISIBLE Z WIDTH

In the previous two sections, we have discussed a series of distinct experimentally measurable quantities which are all closely related to $Z\nu\bar{\nu}$ couplings and the number of active SM neutrinos. In particular, if the SM describes all the processes discussed here, the direct and indirect measurements of the invisible Z width should yield the same result (which may be translated into $N_\nu=3$), while measurements of $g_L^2 + g_R^2$ and g_L discussed in Sec. III should intersect at a single point: $g_L = +1/2$, $g_R = 0$. A statistically significant deviation of any of these measurements from SM predictions would signal that the SM is incomplete, and that new physics is required in order to explain the values of these observables. In particular, it is possible that the direct and indirect measurements of the invisible Z width yield differing results, with the result that the two curves depicted in Fig. 4 would intersect in either two or zero points.

Here, we will briefly discuss new physics mechanisms and/or models that will lead to physically observable effects in the measurements we discussed above. We first discuss several mechanisms for modifying the invisible Z width, concentrating on new physics that would modify the directly and indirectly measured invisible Z width in distinct ways. Then, we argue whether one can construct a model with right-handed neutrino- Z -boson couplings, and further discuss other “applications” of the $g_L \times g_R$ measurement discussed in Sec. III for constraining physics beyond the SM.

A. Direct \times indirect

Several extensions of the SM will lead to an enhancement or suppression of the invisible Z -boson width with respect to

SM expectations. Some of them modify the Z -boson decays in such a way that both the indirect and the direct measurement of the invisible Z width are modified in the same way [i.e., $\Gamma_{\text{inv}}(\text{direct}) = \Gamma_{\text{inv}}(\text{indirect}) \neq \Gamma_{\text{inv}}^{\text{SM}}$]. For example, new decay modes of the Z boson into invisible final states will enhance Γ_{inv} with respect to the SM prediction. One example is the Z -boson decay into a pair of lightest neutralinos in R-parity conserving supersymmetry scenarios, $Z \rightarrow \tilde{\chi}_1^0 \tilde{\chi}_1^0$, when the neutralinos are predominantly B -ino-like.⁹ While such contributions generically enhance the invisible Z width, different new physics effects may lead to a reduction of the magnitude of the $Z\nu\bar{\nu}$ couplings and hence suppress Γ_{inv} . This can be accomplished by assuming, for example, that the SM neutrinos mix slightly with sterile states. With the advent of the NuTeV anomaly [6], which can be explained by reducing the $Z\nu\bar{\nu}$ couplings, this option has recently received a significant amount of attention (see, for example, [8,9]).

Other effects can modify the indirectly measured value of the invisible Z width but not the one obtained directly. One mechanism that will lead to such an effect is the following: assume that there is an exotic decay of the Z boson into final states with some charged and/or neutral particles. Such a decay will not contribute to the direct measurement of the invisible Z width, as events with detector activity other than a single photon are vetoed. On the other hand, if these events fail the selection criteria for leptonic or hadronic Z -boson decays, they will not contribute to Γ_{vis} . Since this new decay mode will increase Γ_{tot} with respect to the SM prediction, $\Gamma_{\text{inv}}(\text{indirect}) = \Gamma_{\text{tot}}^{\text{SM}} + \Gamma_{\text{tot}}^{\text{new}} - \Gamma_{\text{vis}}^{\text{SM}} > \Gamma_{\text{inv}}(\text{direct})$. This might be the case, for example, if the Z boson decays to a pair of neutral particles which themselves decay some centimeters from the interaction point. Another possibility is to introduce an effect that leads to $\Gamma_{\text{tot}}^{\text{measured}} \neq \Gamma_{\text{tot}} = \Gamma_{\text{vis}} + \Gamma_{\text{inv}}$. This will happen, for example, if another resonance is present “on top” of the Z pole [33,34]. Such a resonance will modify the line shape of $e^+e^- \rightarrow f\bar{f}$ (which would no longer be a Breit-Wigner function) and lead to the extraction of an effective total Z -boson width that differs from the “real” total Z -boson width. On the other hand, if this new resonance does not decay into invisible final states, no new contributions to the directly measured value of Γ_{inv} will be present. One possibility of physics hidden by the Z -boson resonance is the s -channel exchange of sneutrinos $\tilde{\nu}$ in R-parity violating supersymmetry [35]. A sneutrino with mass close to the Z -boson mass, $m_{\tilde{\nu}} \approx m_Z$, that primarily decays into $b\bar{b}$ pairs, is not excluded by existing data from LEP and SLD and can lead to deviations in the hadronic Z -boson line-shape parameters compared to the standard Z line-shape parametrization [34].

Finally, some new physics contributions can affect the directly measured value of the invisible Z width but not the one obtained indirectly. The simplest way of accomplishing this is to include new contributions to $e^+e^- \rightarrow$ invisible that

⁹ Z -boson decays into neutralinos with a dominant W -ino or higgsino component are already ruled out by present data.

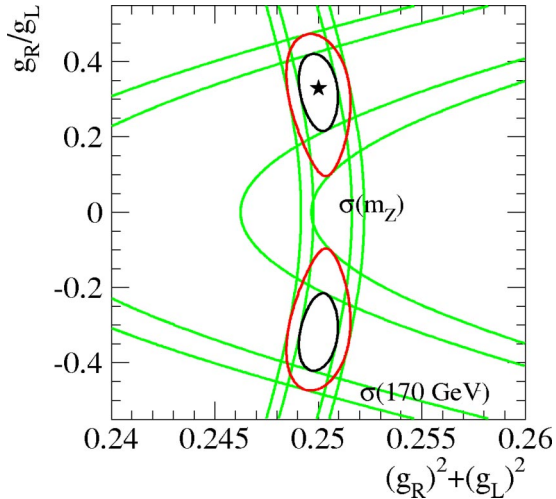


FIG. 6. Projected sensitivity of a linear collider to a nonzero right-handed $Z\nu\bar{\nu}$ coupling $g_R = g_L/3$. As before, the analysis is based on hypothetical measurements of the cross section $e^+e^- \rightarrow \gamma\nu\bar{\nu}$ at the Z-boson mass [$\sigma(m_Z)$] and at $\sqrt{s}=170$ GeV [$\sigma(170 \text{ GeV})$]. The parameters of the underlying scenario are indicated by the star.

are not related to the Z boson. For example, any effective four-fermion interaction similar to $\bar{e}\gamma^\mu e\bar{\nu}\gamma_\mu\nu$ contributes to $e^+e^- \rightarrow \gamma\nu\bar{\nu}$ but does not contribute to Γ_{tot} extracted by the line shape of the Z-boson resonance and hence to Γ_{inv} (indirect). In fact, the most stringent constraints on some of these operators come from $e^+e^- \rightarrow \gamma + \text{invisible}$ [36]. Such a four-fermion operator can be mediated, for example, by the exchange of extra neutral gauge bosons, dubbed Z' bosons. When the Z' boson is relatively light, but weakly coupled so that it forms a narrow resonance, the strongest experimental bounds arise from the radiative return to the Z' pole [37]. It is, therefore, possible that effects of a Z' boson are first discovered in the channel $\gamma\nu\bar{\nu}$. Note that, due to possible interference effects between the Z-boson exchange and the new effective interaction, the directly measured value of Γ_{inv} may be suppressed or enhanced with respect to the SM prediction. Another option is to consider the existence of anomalous $\gamma\nu\bar{\nu}$ couplings, which contribute to the electric and magnetic dipole moments and the charge radii of the neutrinos [25,38,39]. Within the SM, effective $\gamma\nu\bar{\nu}$ interactions are generated at the one-loop level, but have very small values [39,40]. However, loop effects from new physics can induce sizable $\gamma\nu\bar{\nu}$ production rates [25,41]. Such couplings contribute to $e^+e^- \rightarrow \gamma\nu\bar{\nu}$, but do not modify measurements extracted from the Z-boson resonance. Furthermore, other extensions to the SM introduce new invisible particles, Y , that can be produced in $e^+e^- \rightarrow YY\gamma$. These include the Kaluza-Klein gravitons of models with large extra dimensions [42] and super-light gravitinos in supersymmetry scenarios with gauge mediated supersymmetry breaking [43].

Note that in order to enhance the experimental sensitivity to most of the mechanisms outlined in the previous paragraph, one would profit from running at center-of-mass en-

ergies above the Z-boson mass, in order to avoid the “overwhelming presence” of the Z-boson resonance (see discussion in Sec. III). On the other hand, some new physics effects lead to rare single-photon decays of the Z boson, such as $Z \rightarrow \gamma\nu\bar{\nu}$ [44]. In this case, the measurement of the cross section for $e^+e^- \rightarrow \gamma\nu\bar{\nu}$ at the Z pole yields valuable information.

Finally, we emphasize that more information can be obtained by analyzing the missing mass distribution $d\sigma_{\gamma\nu\bar{\nu}}/dM_{\nu\bar{\nu}}$, as described in Sec. III B, and it may be possible to differentiate classes of new physics contributions. As illustrated in Fig. 5, excursions of (g_L, g_R) from the SM values would show up as distinguishable changes in the shape of the missing mass distribution. Another possibility is the existence of a new physics channel, for example, the production of sneutrino pairs ($e^+e^- \rightarrow \tilde{\nu}\tilde{\nu}^*\gamma$), as illustrated in Fig. 5, for the case $M_{\tilde{\nu}}=60$ GeV. For this example, it is assumed that the sneutrinos are of the second or third generation, so that there is no contribution from t -channel chargino exchange, and that the sneutrinos are stable or decay invisibly. Clearly, the shape of the missing mass distribution allows the distinction of this contribution from any new physics effects that modify the properties of the Z boson. In a similar way, the contribution of an extra Z' boson could be identified by a resonance in the missing mass distribution, while the emission of Kaluza-Klein gravitons in large extra dimensions would yield a continuous background without threshold effects.

B. Right-handed neutrino-Z-boson couplings?

In the SM, neutrinos couple only left-handedly to the W and Z bosons. This fact is a direct consequence of the $SU(2)_L \times U(1)_Y$ -gauge symmetry structure of the SM, which fits almost all experimental data beautifully. On the other hand, we should not downplay the importance of directly verifying, experimentally, whether neutrino neutral currents are purely left-handed. Current data allow a right-handed $Z\nu\bar{\nu}$ coupling which is around 40% as large as the left-handed one, while the LC measurement we propose could tighten the bound to about 30%. This should be contrasted with, say, our understanding of $Z\ell\bar{\ell}$ couplings and $W\ell\bar{\nu}$ couplings, which are known (in the worst case) at the few percent level. In Fig. 6 we show an example to illustrate the sensitivity of a linear collider to a nonzero right-handed $Z\nu\bar{\nu}$ coupling. (The same example is also depicted in Fig. 5.) Here, the right-handed coupling is chosen to be one third of the left-handed coupling, which is allowed by current data, while the value for the Z width agrees with the SM prediction. In the setup discussed in Sec. III B, it is possible to discriminate this scenario from the SM at more than the two sigma confidence level. There remains, however, a twofold ambiguity, which is related to the fact that while the sign of g_L can be measured, the sign of g_R remains undetermined.

It is interesting to probe whether there are new physics models that lead to right-handed $Z\nu\bar{\nu}$ couplings. One example is to consider the existence of a heavy Z' boson that mixes slightly with the SM Z boson. In general, Z - Z' mixing

will lead to a shift in the SM Z -boson mass and the SM Z -boson couplings to fermions. It is possible to choose Z' -boson couplings to fermions such that (i) the left-handed $Z\nu\bar{\nu}$ coupling g_L is slightly reduced with respect to its SM value g_L^{SM} , and (ii) a nonzero right-handed $Z\nu\bar{\nu}$ coupling g_R is introduced. If this is done in such a way that $g_L^2 + g_R^2 \simeq (g_L^{SM})^2$, all current experimental constraints can be safely evaded (see Sec. III A).

We have constructed an explicit example, adding to the SM a $U(1)_{Z'}$ gauge symmetry under which leptons and right-handed neutrinos transform. In order to satisfy current experimental constraints and successfully introduce a right-handed $Z\nu\bar{\nu}$ coupling we introduce two extra Higgs bosons. One, transforming nontrivially only under $U(1)_{Z'}$, is responsible for giving the Z' boson a mass. The other, which transforms under both $SU(2)_L$ and $U(1)_{Z'}$, is responsible for inducing mixing between the SM Z boson and the Z' boson.

In the following, Z and Z' denote the mass eigenstates, where the former corresponds to the physical Z boson that has been observed at LEP and other colliders, while the eigenstates of the electroweak gauge group and the extra gauge group are given by Z_1 and Z_2 , respectively. Using this language, we can say that the interference between Z_1 and Z_2 can lead to a reduction of the $Z\nu_L\bar{\nu}_L$ coupling, while a $Z\nu_R\bar{\nu}_R$ coupling is introduced by the Z_2 admixture in the Z boson. Several constraints have to be taken into account, however. First of all, because the Z' couples to charged leptons, it is currently constrained to be very heavy, $m_{Z'} \gtrsim 900$ GeV [2]. Second, in order to induce a relatively large right-handed $Z\nu\bar{\nu}$ coupling, we are required to have either sizable Z - Z' mixing and/or a very large $U(1)_{Z'}$ coupling. Large Z - Z' mixing will imply a significant shift of the Z -boson mass from SM expectations, especially because the Z' is constrained to be very heavy. Third, one should keep in mind that not only are the $Z\nu\bar{\nu}$ couplings modified, but also the $Z\ell\bar{\ell}$ couplings. Taking all of these constraints into account, we are able to find an “existence-proof” example. We choose a $U(1)_{Z'}$ coupling $g' = 3.5$, and set the charges of the left-handed leptons and the right-handed charged leptons to $+1/2$. We also set the charges of the right-handed neutrinos to $+5$.¹⁰ We further set $m_{Z'} = 1$ TeV and the Z - Z' mixing angle to $\sin^2\theta_{ZZ'} = 1.6 \times 10^{-5}$. Under these conditions, the $Z\nu_L\bar{\nu}_L$ coupling g_L is reduced by 3.7%, while a right-handed coupling is generated: $|g_R/g_L| = 0.19$. We further verified that the above mentioned shifts to the $Z\ell\bar{\ell}$ couplings and the Z -boson mass are allowed by the data, and find a fit to Γ_{tot} , $\sin^2\theta_{W,\text{eff}}^\ell$, $\sin^2\theta_{W,\text{eff}}^{\text{had}}$, R_ℓ , and σ_h^0 that is as satisfactory as the SM fit.

We stress that this model is not intended to provide a realistic description of nature, but only to prove the possibil-

ity of “large” right-handed $Z\nu\bar{\nu}$ couplings that are not excluded by existing data. While the specific value, $|g_R/g_L| = 0.19$, we obtained above would still not be detectable at a linear collider, we emphasize that there are other, more complicated, Z' models that induce larger $Z\nu_R\bar{\nu}_R$ couplings. For example, the $Z\nu_L\bar{\nu}_L$ coupling could be further reduced through the addition of higher dimensional operators to the model, thus allowing an increase of the value of the $Z\nu_R\bar{\nu}_R$ coupling to $|g_R/g_L| > 0.3$, which can be distinguished from $g_R = 0$ at more than the two sigma confidence level at a linear collider, as depicted in Fig. 6.

More generally, as briefly alluded to in Sec. III, the g_R need not be a right-handed coupling of the neutrino to the Z boson, but can be interpreted as any coupling of the Z boson to exotic invisible final states. Within the SM, the magnitude of these couplings is best constrained by measuring the invisible Z width at the Z -boson mass, as discussed above. However, by performing the analyses discussed in Sec. III, one is capable of separating the Z -boson coupling to active neutrinos (g_L) from the Z coupling to exotic invisible matter. These analyses allow one to identify models where the g_L coupling is smaller than usual, but is somehow “compensated” by the exotic contribution. If this is the case, the invisible Z -width measurements at the Z -boson mass do not register a discrepancy with respect to the SM, while the measured value of (g_L, g_R) deviates from $(1/2, 0)$ [this is exactly what happens in the $U(1)_{Z'}$ model spelled out above].

V. SUMMARY AND CONCLUSIONS

We have discussed how measurements at e^+e^- colliders provide information on $Z\nu\bar{\nu}$ couplings in distinct ways, allowing the exploration of new physics contributions to the left-handed and right-handed neutrino couplings to the Z boson. The *indirect* measurement of Γ_{inv} is obtained by subtracting the visible partial width from the total width of the Z -boson resonance. It provides a tight constraint on $g_L^2 + g_R^2$. The *direct* measurement of Γ_{inv} comes from measuring the cross section for $e^+e^- \rightarrow \gamma\nu\bar{\nu}$. When this is done at center-of-mass energies around the Z -boson pole mass, it is again possible to constrain the combination $g_L^2 + g_R^2$. At higher center-of-mass energies, however, good sensitivity to g_L is obtained from the interference of the Z -boson and W -boson exchange amplitudes.

We examined published data from LEP in order to constrain g_L and g_R . The strongest constraint by far comes from the indirect value of Γ_{inv} . We have also analyzed data taken at energies above the Z pole (LEP II) in order to extract g_L . Although the result obtained is not particularly precise, in part because only a fraction of the collected data have been analyzed by the LEP collaborations, it establishes the sign of g_L (positive) at the 2σ confidence level. If all existing LEP data were analyzed with the requirement that the missing mass be greater than 100 GeV, we estimate that this analysis would establish g_L with an uncertainty $\delta(g_L) = 0.05$.

Important constraints on $|g_L|$ also come from measure-

¹⁰Here we did not consider anomaly cancellation. We assume that this can be accomplished for example by adding heavy fermions to the theory.

ments of elastic neutrino-electron scattering by CHARM II and LAMPF. Their results agree well with the ones provided by LEP, and with SM predictions. Combining LEP and CHARM II data, the value of the left-handed $Z\nu\bar{\nu}$ coupling is constrained to be $0.45 \leq g_L \leq 0.5$, while the right-handed neutrino couplings to the Z boson are mildly bounded to be $|g_R| \leq 0.2$ at the 2σ level. The NuTeV data can also be used to determine $Z\nu\bar{\nu}$ couplings, in which case a very tight constraint on $|g_L|$ would be obtained. This interpretation, however, rests on several assumptions which are not universally accepted. In our opinion, the elastic neutrino-electron scattering results are cleaner, and we speculate that a new experiment using existing or future neutrino beams should improve substantially the precision with which $|g_L|$ is measured.

A future e^+e^- linear collider could run at center-of-mass energies near the Z -boson pole mass in the so-called ‘‘Giga- Z ’’ option. The integrated luminosities are expected to be much larger than those recorded at LEP, on the order of 50 fb^{-1} . We have estimated how new data taken around the Z -boson pole mass and at $\sqrt{s} = 170 \text{ GeV}$ would improve the constraints already obtained from LEP data. We find that the quality of the indirect measurement of Γ_{inv} would be only modestly improved, while the direct measurement would be performed with greatly improved precision. We estimate that at a linear collider the precision with which the Z -boson width could be directly measured would be comparable to the precision of the indirect measurement. Since both measurements are potentially sensitive to different new physics, a high precision in both is very desirable.

In particular, measurements of $e^+e^- \rightarrow \gamma + \text{invisible}$ at $\sqrt{s} = m_Z$ and $\sqrt{s} = 170 \text{ GeV}$ would be sensitive to values of g_R on the order of $g_L/3$. The data samples should be large enough to warrant a measurement of the cross section as a function of missing mass. Deviations of this differential cross section from the SM prediction would indicate whether g_L , g_R , or both differ from the SM value. The fact that one experiment running at different energies can simultaneously

constrain both g_L and g_R makes the Giga- Z option particularly attractive in this context. The comparison of these two energy regions will provide information analogous to the NuTeV determination of the $Z\nu\bar{\nu}$ couplings.

Finally, we have sketched a variety of new physics scenarios that will impact the measurements of the indirect and direct invisible Z width differently, many of which have been already considered in the literature in various contexts. In summary, by performing both the direct and indirect measurements of the invisible Z width with similar precision, one should be able to distinguish between several different new physics mechanisms, depending on whether the measurements agree or disagree with SM predictions, or whether the two distinct measurements of the invisible Z width agree or disagree with each other. We have also discussed the importance of measuring ‘‘ g_R ’’ as far as constraining new physics. The main reason for this is the fact that while we generally referred to right-handed $Z\nu\bar{\nu}$ couplings, other couplings of the Z boson to exotic, invisible final states are probed in exactly the same way.

We conclude by restating the interesting fact that the current data, in particular the NuTeV anomaly and the LEP measurement of Γ_{inv} , hint at a nonstandard $Z\nu\bar{\nu}$ couplings. Only future experiments can elucidate this issue.

ACKNOWLEDGMENTS

A.d.G. would like to thank the KITP in Santa Barbara and the ICTP in Trieste for their hospitality during, respectively, the early stages and the final stages of this work. M.C. would like to thank the Aspen Center for Physics for its hospitality during the completion of this paper. The work of M.C., A.d.G. and A.F. is supported by the U.S. Department of Energy Contract DE-AC02-76CHO3000. The work of M.S. is supported by U.S. DOE Contract DE-FG02-91ER40684, and by the Illinois Consortium for Accelerator Research, agreement number 228-1001.

-
- [1] ALEPH Collaboration, R. Barate *et al.*, Eur. Phys. J. C **14**, 1 (2000); L3 Collaboration, M. Acciarri *et al.*, *ibid.* **16**, 1 (2000); DELPHI Collaboration, P. Abreu *et al.*, *ibid.* **16**, 371 (2000); OPAL Collaboration, G. Abbiendi *et al.*, *ibid.* **19**, 587 (2001).
- [2] Particle Data Group, K. Hagiwara *et al.*, Phys. Rev. D **66**, 010001 (2002).
- [3] LEP Collaborations and the Line Shape Sub-Group of the LEP Electroweak Working Group, G. Duckeck *et al.*, CERN-EP/2000-153, hep-ex/0101027.
- [4] LEP Electroweak Working Group and SLD Heavy Flavor Working Group, D. Abbaneo *et al.*, CERN-EP/2002-091, hep-ex/0212036.
- [5] For recent analysis see V. Barger, J.P. Kneller, H.S. Lee, D. Marfatia, and G. Steigman, Phys. Lett. B **566**, 8 (2003); S. Hannestad, J. Cosmol. Astropart. Phys. **05**, 004 (2003); R.H. Cyburt, B.D. Fields, and K.A. Olive, Phys. Lett. B **567**, 227 (2003), and references therein.
- [6] NuTeV Collaboration, G.P. Zeller *et al.*, Phys. Rev. Lett. **88**, 091802 (2002); **90**, 239902(E) (2003).
- [7] G.P. Zeller, for the NuTeV Collaboration at the 37th Rencontres de Moriond on Electroweak Interactions and Unified Theories, Les Arcs, France, 2002, hep-ex/0207037.
- [8] A. de Gouvêa, G.F. Giudice, A. Strumia, and K. Tobe, Nucl. Phys. **B623**, 395 (2002); K.S. Babu and J.C. Pati, hep-ph/0203029; E. Ma and D.P. Roy, Phys. Rev. D **65**, 075021 (2002); W. Loinaz, N. Okamura, T. Takeuchi, and L.C. Wijewardhana, *ibid.* **67**, 073012 (2003).
- [9] S. Davidson, S. Forte, P. Gambino, N. Rius, and A. Strumia, J. High Energy Phys. **02**, 037 (2002).
- [10] L3 Collaboration, M. Acciarri *et al.*, Phys. Lett. B **431**, 199 (1998).
- [11] ALEPH Collaboration, D. Buskulic *et al.*, Phys. Lett. B **313**, 520 (1993).
- [12] OPAL Collaboration, R. Akers *et al.*, Z. Phys. C **65**, 47 (1995).
- [13] DELPHI Collaboration, P. Abreu *et al.*, Z. Phys. C **74**, 577 (1997).

- [14] L3 Collaboration, B. Adeva *et al.*, Phys. Lett. B **275**, 209 (1992).
- [15] TESLA Technical Design Report, Part III, edited by R. Heuer, D.J. Miller, F. Richard, and P.M. Zerwas, DESY-2001-011C, hep-ph/0106315; American Linear Collider Working Group Collaboration, T. Abe *et al.*, in Proc. of the APS/DPF/DPB Summer Study on the Future of Particle Physics (Snowmass 2001), edited by R. Davidson and C. Quigg, SLAC-R-570, hep-ex/0106056.
- [16] R. Hawkings and K. Mönig, EPJdirect **1**, 8 (1999).
- [17] M. Winter, in 2nd ECFA/DESY Linear Collider Study (2001), LC-PHSM-2001-016 [<http://www-flc.desy.de/lcnotes/>].
- [18] F.A. Berends, G.J.H. Burgers, C. Mana, M. Martinez, and W.L. van Neerven, Nucl. Phys. **B301**, 583 (1988).
- [19] TESLA Technical Design Report, Part IV, edited by T. Behnke, S. Bertolucci, R.D. Heuer, and R. Settles, DESY-2001-011D.
- [20] T. Ohl, Comput. Phys. Commun. **101**, 269 (1997).
- [21] J. Deutsch, in *Proceedings of the International Symposium WEIN-98*, Santa Fe, 1998 (World Scientific, Singapore, 1999), p. 322; Yu.V. Gapnov and Yu.A. Mostovoi, Phys. At. Nucl. **63**, 1356 (2000) [*Yad. Fiz.* **63**, 1432 (2000)].
- [22] CHARM II Collaboration, P. Vilain *et al.*, Phys. Lett. B **320**, 203 (1994); **335**, 246 (1994).
- [23] V.A. Novikov, L.B. Okun, and M.I. Vysotsky, Phys. Lett. B **298**, 453 (1993).
- [24] LAMPF Collaboration, Phys. Rev. D **47**, 11 (1993).
- [25] M. Hirsch, E. Nardi, and D. Restrepo, Phys. Rev. D **67**, 033005 (2003).
- [26] G. Wilson, in 2nd ECFA/DESY Linear Collider Study (2001), LC-PHSM-2001-009 [<http://www-flc.desy.de/lcnotes/>].
- [27] OPAL Collaboration, G. Abbiendi *et al.*, Eur. Phys. J. C **18**, 253 (2000).
- [28] ALEPH Collaboration, R. Barate *et al.*, Eur. Phys. J. C **28**, 1 (2003); see also Phys. Lett. B **429**, 201 (1998).
- [29] L3 Collaboration, M. Acciarri *et al.*, Phys. Lett. B **470**, 268 (1999).
- [30] DELPHI Collaboration, P. Abreu *et al.*, Eur. Phys. J. C **6**, 371 (1999).
- [31] ATLAS TDR, CERN/LHCC-99-15; E. Accomando *et al.*, Phys. Rep. **299**, 1 (1998).
- [32] LEP Electroweak Working Group and SLD Heavy Flavor and Electroweak Groups, D. Abbaneo *et al.*, CERN-EP/2000-016.
- [33] F. Caravaglios and G.G. Ross, Phys. Lett. B **346**, 159 (1995).
- [34] J. Erler, J.L. Feng, and N. Polonsky, Phys. Rev. Lett. **78**, 3063 (1997).
- [35] S. Dimopoulos and L.J. Hall, Phys. Lett. B **207**, 210 (1988); V.D. Barger, G.F. Giudice, and T. Han, Phys. Rev. D **40**, 2987 (1989).
- [36] Z. Berezhiani and A. Rossi, Phys. Lett. B **535**, 207 (2002).
- [37] T. Appelquist, B.A. Dobrescu, and A.R. Hopper, Phys. Rev. D **68**, 035012 (2003).
- [38] J.F. Nieves, Phys. Rev. D **26**, 3152 (1982); R.E. Shrock, Nucl. Phys. **B206**, 359 (1982).
- [39] J. Bernabéu, L.G. Cabral-Rosetti, J. Papavassiliou, and J. Vidal, Phys. Rev. D **62**, 113012 (2000).
- [40] V.M. Dubovik and V.E. Kuznetsov, Int. J. Mod. Phys. A **13**, 5257 (1998).
- [41] N. Tanimoto, I. Nakano, and M. Sakuda, Phys. Lett. B **478**, 1 (2000).
- [42] G.F. Giudice, R. Rattazzi, and J.D. Wells, Nucl. Phys. **B544**, 3 (1999); E.A. Mirabelli, M. Perelstein, and M.E. Peskin, Phys. Rev. Lett. **82**, 2236 (1999).
- [43] S. Dimopoulos, S. Thomas, and J.D. Wells, Nucl. Phys. **B488**, 39 (1997); J.L. Lopez, D.V. Nanopoulos, and A. Zichichi, Phys. Rev. D **55**, 5813 (1997); A. Brignole, F. Feruglio, and F. Zwirner, Nucl. Phys. **B516**, 13 (1998); **B555**, 653(E) (1999).
- [44] M.A. Pérez, G. Tavares-Velasco, and J.J. Toscano, hep-ph/0305227.